SIMPLIFIED SEISMIC MODELLING OF REINFORCED CONCRETE FLEXURAL MEMBERS

Maged A. Youssef, Ph.D., P.Eng., Assistant Professor

Mizanur Rahman, M.E.Sc., P.Eng., Ph.D. Candidate

Corresponding Author: Dr. M.A. Youssef, P.Eng.

The University of Western Ontario, Department of Civil and Environmental Engineering, London, ON N6A 5B9, CANADA.

Phone: 519-661-2111 Ext. 88661

Fax: 519-661-3779

E-mail:myoussef@eng.uwo.ca

Word Count: 3498

Number of tables 1

Number of Figures 17

KEYWORDS: Concrete structures, Mathematical Modelling, Seismic Engineering

SYNOPSIS

The need for simplified models that can accurately represent the behaviour of structures is increasing. Engineers need such models to assess and/or to design structures using pre-specified performance measures. In this paper, the abilities of a previously developed model for reinforced concrete flexural members are significantly enhanced. The model represents a member by an elastic element and two-inelastic end elements. Each inelastic element consists of three-concrete and three-steel springs. A rational approach to calculate the properties of these springs is developed. The approach includes a simplified method to account for slippage of reinforcing bars. The model allows identifying the localized damage (concrete cracking, reinforcement yielding, concrete crushing, or bond-slip failure) responsible for any change in the overall performance of an RC frame. To illustrate the use of this approach and to validate its predictions, two cantilever columns are modeled and analyzed under monotonic and cyclic loadings.

Introduction

Seismic analysis of Reinforced Concrete (RC) framed structures requires realistic analytical procedures to produce reasonably accurate simulations of behaviour[1]. Such procedures must have the ability to predict different failure modes including: concrete crushing and bond-slip failure and thus allow engineers to predict the expected damage to an RC structure under extreme cases of loading.

Lai et al.[2] have developed an effective three-dimensional analytical model (multi-spring model) to predict the inelastic hysteretic and stiffness degradation behaviour of RC members subjected to axial load and biaxial bending. The parameters of the model are based on empirical equations

and thus are valid for a limited number of applications. Also, representation of strength deterioration due to different failure modes is not included in the model.

Based on Lai's[2] model, Youssef and Ghobarah[3] developed a macro model to account for strength deterioration due to bond slip and crushing of concrete. A beam or a column is represented by an elastic element and two inelastic end elements, as shown in Fig. 1. Each inelastic element consists of three concrete and three steel springs. They represent the stiffness of the effective reinforcing steel bars and the effective concrete. The springs are connected by rigid frame elements as shown in Fig. 1. The model included a number of limitations.

1. The capacity of the edge concrete springs is calculated based on the concrete compressive force at ultimate condition. This is only valid for sections with low axial forces.
2. Concrete stress-strain relationships are linearly transformed to force-deformation relationships using the expected ultimate capacity and ultimate deformation of the edge concrete springs. Such a method may not accurately capture the actual behaviour of RC members at different load stages.
3. The capacity of the central concrete spring is calculated as the difference between the capacity of the entire section and the edge springs. The distance between the edge-springs is calculated by equating the ultimate moment resisted by the edge steel and concrete springs with that of the actual section. Such a method will not guarantee that the moments are equal at other stages of loading.
4. The stiffnesses, capacities, and locations of the steel springs are based on their expected slip, which reduce the accuracy of the model when bond-slip is not governing.

The main objective of the current study is to develop a simplified model for the simulation of RC flexural members subjected to reversed cyclic loading to address the need to accurately predict

the peak strength and ductility of RC structures. This is achieved by developing a rational approach for the computation of the properties of the multi-spring model.

Proposed model

In this model, a beam or a column is represented by an elastic element and two inelastic end elements, as shown in Fig. 1. The elastic element properties are taken as those for the concrete section before cracking. Each inelastic element consists of three concrete and three steel springs. The position of the edge concrete and steel springs is chosen to coincide with the tensile and compressive reinforcements. The remaining two springs are positioned at the centre of the section. The properties of each spring are defined using the following-steps.

1. Material models

The uniaxial stress-strain relationship for concrete in compression is chosen to follow the model of Scott et al.[4]. The monotonic concrete stress-strain relation in compression, shown in Fig. 2, is described as follows:

$$f_c = K_h f_c' \left[2.\left(\frac{\varepsilon_c}{\varepsilon_o}\right) - \left(\frac{\varepsilon_c}{\varepsilon_o}\right)^2 \right] \qquad \varepsilon_c \le \varepsilon_o \qquad (1a)$$

$$f_c = K_h f_c' \left[1 - Z_c\left(\varepsilon_c - \varepsilon_o\right)\right] \qquad \ge 0.2K_h f_c' \qquad \varepsilon_c \ge \varepsilon_o \qquad (1b)$$

Where,

f_c = concrete compressive stress (MPa).

f_c' = concrete compressive strength (MPa).

ε_c = concrete strain.

K_h = confinement factor.

ε_o = concrete strain at maximum stress.

Z_c = slope of the strain-softening branch.

The uniaxial stress-strain relationship for concrete in tension is modeled by a linear branch until reaching the cracking stress, $f_{cr} = 0.33\sqrt{f_c'}$, and then follows a softening branch. The modulus of elasticity of the linear branch is taken equal to that of the compressive branch at zero strain. The softening branch is described by the following formula[3].

$$f_t = f_{cr} \cdot \left[0.95\, e^{-1000\left(\varepsilon_c - \varepsilon_{cr}\right)} + 0.05 \right] \tag{1c}$$

Where,

f_t = concrete tensile stress

ε_{cr} = concrete cracking strain

The chosen uniaxial stress-strain relationship for reinforcing bars is shown in Fig. 3 and it follows a bilinear curve in both tension and compression. Modulus of elasticity E_s, yield stress f_y, and hardening ratio r, defining the post yielding stiffness $r.E_s$, are chosen to be equal for both tension and compression.

2. Sectional analysis

Concrete sectional behaviour is defined using a fibre model. The section is divided into a number of discrete fibres, as shown in Fig. 4. Using uniaxial stress-strain relationships for each fibre and taking into account equilibrium and kinematics, the mechanical behaviour of the section is analyzed. The relationship between the incremental changes in axial strain $\Delta\varepsilon_c$, curvature $\Delta\Phi$, applied moment ΔM, and axial force ΔP can be written as:

$$\begin{pmatrix} \Delta M \\ \Delta P \end{pmatrix} = \begin{pmatrix} \sum_{i=1}^{n} E_i \times A_i \times y_i^2 & -\sum_{i=1}^{n} E_i \times A_i \times y_i \\ -\sum_{i=1}^{n} E_i \times A_i \times y_i & \sum_{i=1}^{n} E_i \times A_i \end{pmatrix} \times \begin{pmatrix} \Delta \Phi \\ \Delta \varepsilon_c \end{pmatrix} \quad (2)$$

Where,

E_i = modulus of elasticity of layer i.

A_i = area of layer i.

y_i = distance between the centre of gravity of layer i and the centre of gravity of the section.

For a given axial load and an increasing moment the sectional behaviour is obtained in two stages. In the first stage, the axial force is applied in an incremental way while moment and curvature are kept equal to zero. In the second stage, axial load is kept constant at the desired level that was reached in stage 1 and the applied curvature is increased from zero to a specified value.

3. Forces in steel and concrete springs

For a given axial load and moment, the equivalent forces in the steel springs can be evaluated from sectional analysis. No modification for these forces is needed, as the edge springs are chosen to coincide with compressive and tensile steel reinforcement. Regarding equivalent forces in the three concrete springs, a rational approach is developed to divide the concrete compressive and tensile forces among them.

Stage I: (Strain at location of concrete spring number one is less than the cracking strain)

For an incremental increase of the applied moment (ΔM), the incremental change in the forces of the steel springs (ΔP_{S1}, ΔP_{S2}, ΔP_{S3}) can be evaluated from the sectional analysis. The incremental

change in the forces of the concrete springs (ΔP_{C1}, ΔP_{C2}, ΔP_{C3}) can be determined from the change in the concrete area represented by each spring (ΔA_{C1}, ΔA_{C2}, ΔA_{C3}).

The area of a given concrete section is constant and thus the relationship between the incremental change in the concrete areas ΔA_{C1}, ΔA_{C2}, ΔA_{C3} representing springs 1, 2 and 3, respectively can be written as:

$$\Delta A_{C1}+\Delta A_{C2}+\Delta A_{C3} = 0 \qquad (3a)$$

Assuming perfect bond between steel and concrete, coinciding steel and concrete springs will have the same deformation.

$$\Delta_{Ci} \text{ (concrete)} = \Delta_{Si} \text{ (steel)} \qquad (i = 1, 2, 3) \qquad (3b)$$

The relationship between these incremental deformations and the stiffnesses of the springs (K_{Ci} or K_{Si}) can be written as,

$$\Delta_{Ci} = \frac{\Delta P_{Ci}}{K_{Ci}} \quad \text{and} \quad \Delta_{Si} = \frac{\Delta P_{Si}}{K_{Si}} \qquad (3c)$$

Ignoring the variation of modulus of elasticity of concrete over the depth of concrete area represented by each concrete spring, the stiffness of the concrete and steel springs can be represented by: $\frac{E_{ci} A_{ci}}{L_{ci}}$ and $\frac{E_{si} A_{si}}{L_{si}}$, respectively. E_{ci} and E_{si} are the modulus of elasticities of concrete and steel at the locations of the springs. Further assuming that the length represented by the steel (L_{si}) and concrete (L_{ci}) springs is the same, the following relationship can be written:

$$\frac{K_{Ci}}{E_{Ci} A_{Ci}} = \frac{K_{Si}}{E_{Si} A_{Si}} \qquad (i = 1, 2 \text{ or } 3) \qquad (3d)$$

The incremental changes in the internal compressive and tensile forces (ΔP_{CC}, ΔP_{CT}) in the concrete section, evaluated by the sectional analysis, is related to the incremental change in the forces of the concrete springs by the following equation:

$$\Delta P_{CC} + \Delta P_{CT} = \Delta P_{C1} + \Delta P_{C2} + \Delta P_{C3} \tag{3e}$$

By substituting the equations (3b) and (3c) into equation (3e), the following equation can be obtained:

$$\Delta P_{CC} + \Delta P_{CT} = \frac{E_{C1}(A_{C1-prev} + \Delta A_{C1})}{E_{S1} A_{S1}} \Delta P_{S1} + \frac{E_{C2}(A_{C2-prev} + \Delta A_{C2})}{E_{S2} A_{S2}} \Delta P_{S2} + \frac{E_{C3}(A_{C3-prev} + \Delta A_{C3})}{E_{S3} A_{S3}} \Delta P_{S3} \tag{3f}$$

Where, $A_{C1\text{-}prev}$, $A_{C2\text{-}prev}$ and $A_{C3\text{-}prev}$ are the concrete areas represented by springs 1, 2 and 3, respectively in the previous step.

To ensure that the equivalent spring system will have the same moment as that of the modeled section, the following moment equilibrium equation can be written:

$$\Delta P_{CC} \cdot \bar{y}_C - \Delta P_{CT} \cdot \bar{y}_T = \frac{E_{C1}(A_{C1-prev} + \Delta A_{C1})}{E_{S1} A_{S1}} \Delta P_{S1} Z - \frac{E_{C3}(A_{C3-prev} + \Delta A_{C3})}{E_{S3} A_{S3}} \Delta P_{S3} Z \tag{3g}$$

Where, $\bar{y}_C$, $\bar{y}_T$ and Z are the distances between the middle spring and the internal concrete compressive force, the internal concrete tensile force, and the exterior springs, respectively.

For a given incremental change in the forces of the steel springs, ΔA_{C1}, ΔA_{C2}, and ΔA_{C3} can be determined by solving equations (3a), (3f), and (3g). The incremental change in the force of each concrete spring can then be evaluated using equations (3b), (3c), and (3d).

Stage II: (Cracking strain is less than concrete strain at location of spring number one but is greater than concrete strain at location of spring number two)

At this stage, concrete strain at location of spring one reaches the cracking strain and consequently the tangential modulus drops suddenly from a high positive value to a high negative value. Such a sudden change magnifies any small error resulting from the approximations behind equation (3d). Therefore, it has been chosen to separate the compressive

and tensile behaviour. Spring one is chosen to represent the concrete section tensile behaviour. The incremental change in its force at any step is given by the following equation

$$\Delta P_{C1} = \Delta P_{CT} \frac{\text{Distance from c.g. of the tensile force to the middle spring}}{Z} \quad (3h)$$

The incremental change in the sectional compressive force is represented by spring 2 and 3. The force in spring 3 can be evaluated from the following moment equilibrium equation.

$$\Delta P_{CC}\, \bar{y}_C = \Delta P_{C3}\, Z \quad (3i)$$

The force in spring two would be the difference between ΔP_{CC} and $\Delta P_{C3.}$

Stage III: (Strain at location of springs one and two is greater than the cracking strain)

At this stage, the concrete strain at location of the middle spring also reaches the cracking strain. For the same reason as discussed in stage II, compressive and tensile behaviour has been separated. Spring three represents the concrete section compressive behaviour whereas springs one and two represent the concrete section tensile behaviour. The incremental change in its force at any step is given by the following equation:

$$\Delta P_{C3} = \Delta P_{CC} \frac{\text{Distance from c.g. of the compressive force to the middle spring}}{Z} \quad (3j)$$

The force in spring one can be evaluated from the following equation:

$$\Delta P_{CT}\, \bar{y}_T = \Delta P_{C1}\, Z \quad (3k)$$

The force in spring two will be equal to the difference between ΔP_{CT} and ΔP_{C1}.

4. Deformations and stiffness

The total deflection (δ_{total}) of any flexural member can be calculated at different load stages by integrating the curvature obtained using sectional analysis along the member length. This

deflection can be used to calculate the deformation of concrete and steel springs after subtracting the elastic component of the deflection.

Fig. 5 shows the deflected shape of a cantilever member, and the curvature distribution in the elastic and inelastic stages. The angle θ, defining the member inelastic rotation can be calculated from the following equation:

$$\theta = \frac{\delta_{total} - \delta_{elastic\ deformation}}{L} \tag{4a}$$

Where, L is the member length.

Assuming a cantilever member, θ can be written as:

$$\theta = \frac{1}{L}\left(\delta_{total} - \frac{PL^3}{3E_c I_g}\right) \tag{4b}$$

The difference between deformations of springs one and three is given by

$$\Delta_{s3} - \Delta_{s1} = \Delta_{c3} - \Delta_{c1} = 2\,Z\theta \tag{4c}$$

Assuming that both springs has the same stiffness, this will lead to:

$$K_{S1} = K_{S3} = \frac{P_{S3} - P_{S1}}{2.Z.\theta} \tag{4d}$$

The difference between the deformations of springs one and two is used to define the stiffness of spring two.

$$\Delta_{s2} - \Delta_{s1} = \Delta_{c2} - \Delta_{c1} = Z\theta \tag{4e}$$

$$K_{S2} = \frac{P_{S2}}{\frac{P_{S1}}{K_{S1}} + Z\theta} \tag{4f}$$

The stiffnesses of the steel springs are evaluated using equations (4d) and (4f). These stiffnesses can be used to calculate the expected deformations of the concrete springs and thus their stiffnesses as follows:

$$\Delta_{ci} = \Delta_{si} = \frac{P_{Si}}{K_{Si}} \qquad (i = 1, 2, 3) \tag{4g}$$

$$K_{Ci} = \frac{P_{Ci}}{\Delta_{ci}} \qquad (i = 1, 2, 3) \tag{4h}$$

It should be noted that the methodology defined above, will result in wrong estimates of the member axial deformation, which are usually very small for typical moment frames and do not affect the overall behaviour.

5. Bond slip

Experimental studies have shown that under lateral loading, the most unfavourable bond condition exist in the beam-to-column connections leading to significant fixed end rotations. It is therefore crucial to consider these deformations in the analysis of the RC frames.

The overall shape of the local bond stress–slip constitutive model used in this study is shown in Fig 6. The slip and stress values defining the curve can be approximately related to the ultimate bond stress τ_1, and the corresponding slip S_1, using the following equations[3]:

$$S_2 \cong 3S_1 \qquad S_3 \cong 10S_1 \qquad \tau_3 \cong \frac{\tau_1}{3} \tag{5}$$

The method described by Giuriani and Plizzuri[5] can be adopted to calculate τ_1 and S_1. This method takes into account the confining action of different amounts of transverse reinforcement. It is valid in areas affected by flexural cracking and thus can be used for splices located outside the beam–to–column joint. For splices located within the beam–to–column joint, the average values of τ_1 and S_1 for confined or unconfined concrete that were reported by Eligenhausen et al.[6] can be used.

The local bond stress–slip constitutive model defined above can be used to solve the equilibrium, compatibility and constitutive relations of a bar embedded into concrete using one of the

approaches available in the literature [3, 7, 8]. This will result in defining the steel stress–slip relationship.

6. Modified stiffness of steel springs

The steel bond stress–slip relationship obtained in the previous section is used to adjust the stiffnesses of the steel springs to account the bond-slip. The resulting decrease in the stiffnesses of the steel springs is expected to increase the demand on the concrete springs.

7. Force deformation relationships

The purpose of this section is to find equations to represent the force-deformation relationships of the concrete and steel springs, defined in the previous sections. These equations will simplify formulating the spring elements.

Steel springs

The force deformation relationship of a typical steel spring is modeled using the curve shown in Fig. 7. Each of the tensile and compressive curves is divided into three parts: elastic, elasto-plastic and softening. K_{St} and K_{Sc} are the stiffnesses of the elastic part in tension and compression respectively. Softening part of the curve is mainly due to bond-slip softening and the spring force P_S at any displacement d_S for this zone is given by the following equation[3]:

$$P_S = P_{SU}\left(R_{SO} + \frac{1 - R_{SO}}{1 + \alpha_S(d_S - d_{SU})}\right) \tag{7a}$$

Where,

R_{SO} = Ratio between the residual force in the steel bars after complete slippage occurs and the maximum load P_{SU}.

α_S = softening factor

The values of K_S, P_{sy}, P_{su}, d_{su}, R_{SO}, and α_S in compression (c) and tension (t) are determined using the results of the previous sections.

Concrete springs

Fig. 8 shows the force deformation relationship used to model the concrete springs. Each of the tensile and compressive curves is divided into three parts. While part I represents the linear elastic behaviour, parts II and III represent the non-linear behaviour. Each non-linear part is approximated by a fourth order polynomial of the form:

$$P_c = k_1 . d_c^4 + k_2 d_c^3 + k_3 d_c^2 + k_4 d_c + k_5 \quad (7b)$$

The limits of each part, the elastic stiffnesses, and the constants K_1, K_2, K_3, K_4, and K_5 can be determined from the results of the previous sections.

8. Hysteretic rules

The concrete spring hysteretic model proposed by Youssef and Ghobarah[3] is adopted in this study. Regarding the steel spring, a typical elasto-plastic hysteretic model is modified to account for possible bond slip degradation, and unequal tensile and compressive stiffnesses. Two possible cycles are shown in Fig. 9. Loading starts in the positive direction with stiffness K_{St} until the yield force P_{SYt} is reached where the post yield curve is followed. The load direction is then reversed and unloading proceeds with the same initial stiffness K_{St}. When loading start in the negative direction, the stiffness changes to the compressive stiffness K_{Sc}. This will continue until reaching point A_1, lying on the extension of the compressive post-yielding branch. The same procedure will be repeated when unloading from the compressive branch occurs. In the second

cycle, it is assumed that the inelastic tensile deformation reached d_{st} and thus tensile bond-slip failure occurred. The same performance will occur in the compression zone when the inelastic deformation reaches d_{sc}.

Examples

The methodologies to obtain forces and deformation in steel and concrete springs are applied to two reinforced concrete columns (Specimens S1 and S3) tested by Ghobarah et al.[9]. This was done to validate the model and to provide details of the various steps described in this paper. The envelope curves of the steel and concrete springs are then incorporated into a general-purpose non-linear structural analysis program PC-ANSR to validate the proposed model.

Description of the specimens

Specimens S1 and S3, shown in Fig. 10, represent the sections of cantilever columns. They were designed by Ghobarah et al.[9] to represent existing structures designed according to NBCC[10] (1960) and new structures designed according to recent seismic codes[11]. Both specimens were reinforced with longitudinal reinforcement of 12M15 bars (16 mm nominal diameter) with yield strength of 437 MPa. Concrete strength was 24 MPa. Development length used for the longitudinal bars in both specimens was 600 mm. The only difference in reinforcement between specimens S1 and S3 was the tie reinforcement, which is shown in Fig. 10. A constant axial load of 505 kN was applied to both specimens. The cyclic lateral load was applied at a distance 2550 mm from the base of the column.

Sectional Analysis

Sectional analysis for both specimens is performed following the procedures described in section 3. For each specimen an axial load of 505 kN is applied, which is followed by incremental increase of curvature while keeping the axial load constant. The resulting moment curvature diagram for both specimens is shown in Fig. 11. The moment-curvature diagram for specimen S3 shows more ductile behaviour than specimen S1.

Force deformation of concrete and steel spring

Following the methodology described in sections 4 and 5 the force-deformation relationships for both steel and concrete springs are obtained. The force displacement relationships of concrete springs for specimens S1 and S2 are shown in Fig. 12. The coefficients defining the equation for each portion of the non-linear curve for both specimens S1 and S3 are calculated and are shown in Table 1.

Fig. 13 shows the force-displacement relationships of steel springs for both specimens. The tensile and compressive curves are divided into three parts. The methodology proposed by Giuriani and Plizzari[5] to predict τ_1 and s_1 was adopted, as the splices were located outside the foundation where flexural cracks are expected. Knowing the local bond stress curve allows defining the steel stress-slip relationships. These relationships are given in Fig.14 for specimens S1 and S3. The force-deformation relationships of the steel springs are corrected using these relationships and are shown in Fig. 13.

Monotonic Behaviour

Both specimens are subjected to increasing lateral load while keeping the axial load constant at 505 kN. To judge on the importance of bond-slip deformations, each specimen is analyzed twice. The only difference between the two analyses is the steel springs force-deformation relationships as both before and after considering bond-slip deformations are used. Fig. 15 shows the monotonic load-displacement behaviour of both specimens.

The significant reduction in load after reaching maximum load due to bond slip for specimen S1 is observed. Specimen S3 does not show the significant load reduction, as it was designed according to latest code, which considers improved confinement of longitudinal reinforcement. The monotonic curves are characterized by point A (tensile concrete spring reaches the cracking strain), point B (tensile steel spring yields), point C (compressive concrete spring reaches its maximum strength), Point D (tensile concrete spring looses its capacity), and point E (tensile steel spring fails due to bond-slip softening). The obtained load-deflection curve shows the capability of the model to predict the behaviour of reinforced concrete sections up to failure.

Cyclic Behaviour

Each specimen was subjected to reversed cycles of deformation-controlled cycles matching the experiments[9]. The experimental and analytical results are shown in Figs. 16 and 17. Specimen S1 behaviour is greatly affected by the inclusion of bond-slip. The specimen shows bond slip softening at a displacement of about 100 mm. Because of the symmetry of the specimen, the analytical results are the same in the negative and positive loading directions. The specimen behaviour is matching the experimental one in terms of stiffness and strength degradation in one of the loading directions (negative quad). In the other loading direction, the experiment shows

higher degradation than that predicted by the model. This might be attributed to variability in concrete cover. Inclusion of bond-slip deformations has minor effect on the behaviour of specimen S3. Comparing Figs. 17a and 17b, it is clear that the model predictions in terms of stiffness degradation, failure mode are sufficiently accurate.

SUMMARY AND CONCLUSIONS

A previously developed macro model for the representation of the inelastic behaviour of RC flexural members has been greatly enhanced. In this model, a flexural member is modeled using an elastic beam element and two inelastic end elements. A new rational approach is developed to calculate the properties of the three-steel and three-concrete springs composing the inelastic element. The approach involves calculating the moment curvature relationship of the concrete section using fibre model. Using compatibility, and equilibrium, the forces of concrete and steel springs are calculated at different load stages. Their deformations and stiffnesses are then calculated by integrating the curvature diagram over the member length. A simplified method to account for the slippage of reinforcing bars is also introduced.

Two reinforced concrete cantilever column are modeled and analyzed using the proposed model under monotonic and cyclic loading. The model predictions are in good agreement with the experimental results. The analysis proves that the model is able to predict the damage due to: concrete cracking, concrete crushing, reinforcement yielding, and bond slippage.

It should be noted that the developed element is limited to flexural behaviour and cases with small variations in the axial force. Future studies are needed to include shear deformations and axial force variations.

ACKNOWLEDGMENTS

The authors would like to acknowledge the financial support provided by the Natural Science and Engineering Research Council of Canada ((NSERC), and the Institute for Catastrophic Loss Reduction of university of western Ontario (ICLR).

REFERENCES

1. Palermo D., and Vecchio F.J., Compression Field Modeling of Reinforced Concrete Subjected to Reversed Loading: Formulation. ACI Structural Journal, 2003, 100, 5, 616-625.
2. Lai S.S., Will G.T., and Otani S., Model for Inelastic Biaxial Bending of Concrete Members. Journal of Structural Engineering-ASCE, 1984, 110, 11, 2563-2584.
3. Youssef M. and Ghobarah A., Strength Deterioration due to Bond Slip and Concrete Crushing in Modeling of Reinforced Concrete Members. ACI Structural Journal, 1999, 96, 6, 956-966.
4. Scott B.D., Park R., and Priestley M.J.N., Stress-Strain Behavior of Concrete Confined by Overlapping Hoops at Low and High Strain Rates. ACI Journal, 1982, 79, 1, 13-27.
5. Giuriani E. and Plizzari G.A., Interrelation of Splitting and Flexural Cracks in Reinforced Concrete Beams. Journal of Structural Engineering-ASCE, 1998, 124, 9, pp. 1032-1040.
6. Eligenhausen R., Popov E.P., and Bertero V.V., Local bond stress-slip relationships of deformed bars under generalized excitations. Report No. EERC 83/23, University of California, Berkeley, 1983.
7. Filippou F.C., Popov E.P., and Bertero V.V. Effect of Bond Deterioration on Hysteretic Behavior of Reinforced Concrete Joints. Report No. UCB/EERC 83/19, University of California, Berkley, 1983.
8. Monti G., Filippou F.C., and Spacone E. Finite Element for Anchor Bars Under Cyclic Load Reversals. Journal of Structural Engineering-ASCE, 1997, 123, 5, 614-623.
9. Ghobarah A., Biddah A., and Maghoub M., Rehabilitation of Reinforced Concrete Columns using Corrugated Steel Jacketing. Journal of Earthquake Engineering, 1997, 1, 4, 651-673.
10. NBCC, National Building Code of Canada, Third Edition, National research Council, Ottawa, Ontario, 1960.

11. CSA A23.3-94, Design of Concrete Structures for Buildings, Canadian Standards Association, Rexdale, Ontario, 1994.

Nomenclature:

A_{Ci}	area of concrete spring i.
$A_{Ci\text{-}prev}$	area represented by concrete spring i in the previous step.
A_i	area of layer i.
A_{Si}	area of steel spring i.
b	width of cross section.
d_c	displacement of concrete spring.
d_S	displacement of steel spring.
d_{Sc}	difference between displacement at peak compressive force and displacement at compressive yielding for the steel spring.
d_{St}	difference between displacement at peak tensile force and displacement at tensile yielding for the steel spring.
d_{suc}	compressive displacement at peak compressive force for the steel spring.
d_{sut}	tensile displacement at peak tensile force for the steel spring.
E_c	modulus of elasticity of concrete ($E_c = 4500.\sqrt{f'_c}$ MPa).
E_{ci}	modulus of elasticity of concrete at the location of spring i.
E_i	modulus of elasticity of layer i.
E_s	modulus of elasticity of reinforcing bars.
E_{si}	modulus of elasticity of steel at the location of spring i.
f_c	concrete compressive stress (MPa).
f'_c	concrete compressive strength (MPa).
f_{cr}	concrete tensile strength (MPa).
f_t	concrete tensile stress.
f_y	yield strength of reinforcing bars.
f_{yh}	yield strength of transverse reinforcement (MPa).
h	height of cross section.
h'	width of the concrete core measured to outside of the ties.
I_g	gross moment of inertia of the concrete section.
k_1, k_2, k_3, k_4, k_5	concrete spring parameters.
K_{Ci}	stiffness of concrete spring number i.
K_h	confinement factor ($K_h = 1 + \frac{\rho_s f_{yh}}{f'_c}$)
K_{Sc}	elastic compressive stiffness of the steel spring.
K_{Si}	stiffness of steel spring number i.
K_{St}	elastic tensile stiffness of the steel spring.
L	length of the flexural member.
L_{ci}	plastic length represented by concrete spring i.
L_{si}	plastic length represented by steel spring i.
P	Applied load.
P_c	force in the concrete spring at displacement d_c.
P_{Ci}	force in concrete spring number i.
P_S	force in the steel spring at displacement d_S.
P_{Si}	force in steel spring number i.
P_{SUc}	ultimate compressive force of the steel spring.
P_{SUt}	ultimate tensile force of the steel spring.

P_{syc} compressive yield force of steel spring.

P_{syt} tensile yield force of steel spring.

r hardening ratio (ratio between the post yielding and initial modulus of elasticities).

R_{SO} Ratio between the residual force in the steel bars after complete slippage occurs and the maximum load P_{SU}.

S_1, S_2, S_3 slip values defining the shape of the bond stress-slip relationship.

S_h centre-to-centre spacing of the ties or hoop sets.

$\bar{y}_C$ distance between the middle spring and the internal concrete compressive force.

$\bar{y}_T$ distance between the middle spring and the internal concrete tensile force.

y_i distance between the centre of gravity of layer i and the centre of gravity of the concrete section.

Z distance between the middle spring and the exterior springs.

Z_c slope of the strain-softening branch $\left(Z_c = \frac{0.5}{\frac{3+0.29f_c'}{145f_c'-1000} + 0.75\rho_s\sqrt{\frac{h'}{S_h}} - 0.002K_h} \right)$.

$\Delta\phi$ incremental change in section curvature.

$\Delta\varepsilon_c$ incremental change in the section central axial strain.

ΔA_{Ci} incremental change in the areas represented by concrete spring i.

Δ_{Ci} axial deformation of concrete spring number i.

ΔM incremental change in the moment acting on the section.

ΔP incremental change in the axial force acting on the section.

ΔP_{CC} incremental change in the internal compressive concrete force.

ΔP_{Ci} incremental change in the force of concrete spring i.

ΔP_{CT} incremental change in the internal tensile concrete force.

ΔP_{Si} incremental change in the force of steel spring i.

Δ_{Si} axial deformation of steel spring number i.

α_S softening factor.

$\delta_{elastic\ deformation}$ elastic part of the total deflection.

δ_{total} maximum total deflection of a flexural member.

ε_c concrete strain.

ε_{cr} concrete cracking strain.

ε_o concrete strain at maximum stress ($\varepsilon_o = 0.002 \times K_h$).

θ inelastic rotation.

ρ_s ratio of the volume of transverse reinforcement (ties) to the volume of concrete core measured to outside of the ties.

τ bond stress.

τ_1 ultimate bond stress.

τ_3 residual bond stress.

List of Tables:

List of Figures:

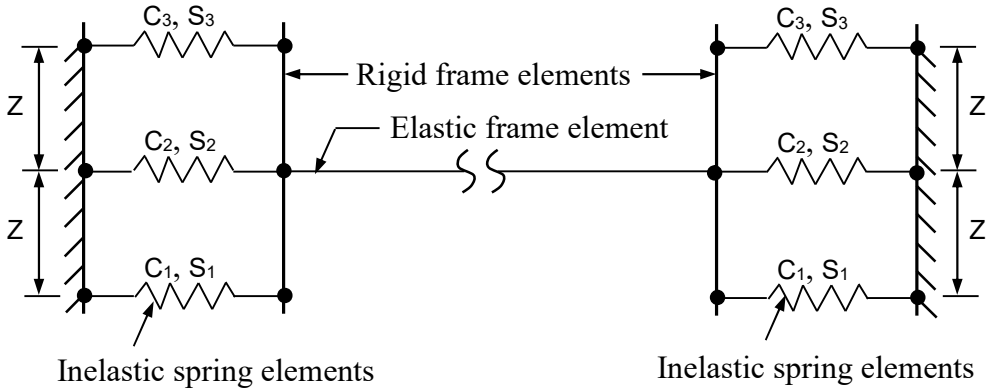

Fig. 1. Beam / Column element.

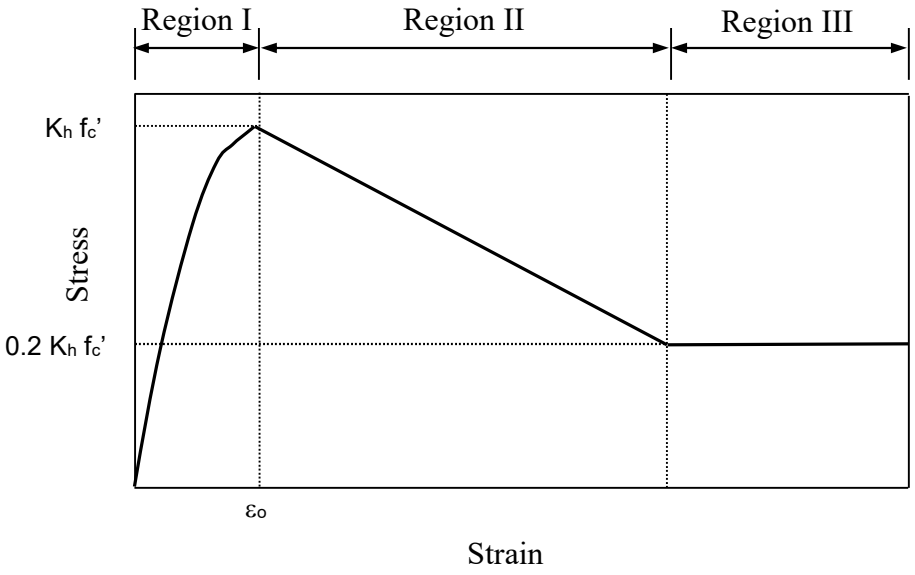

Fig. 2. Concrete stress-strain relationship.

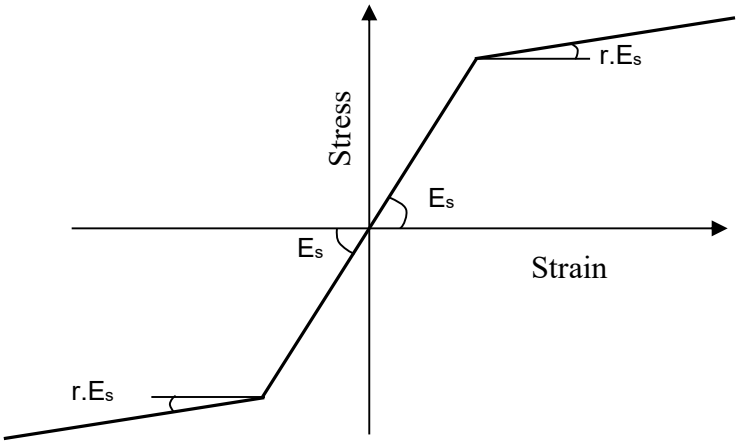

Fig. 3. Steel material model.

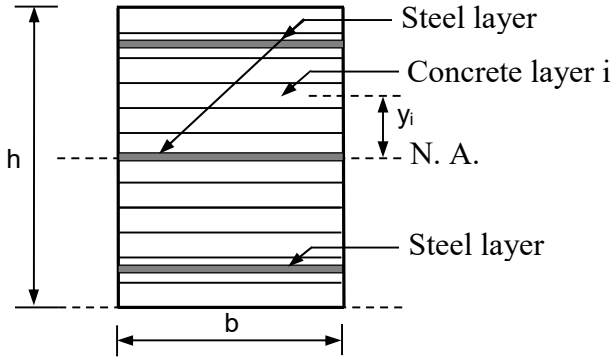

Fig. 4. Concrete section.

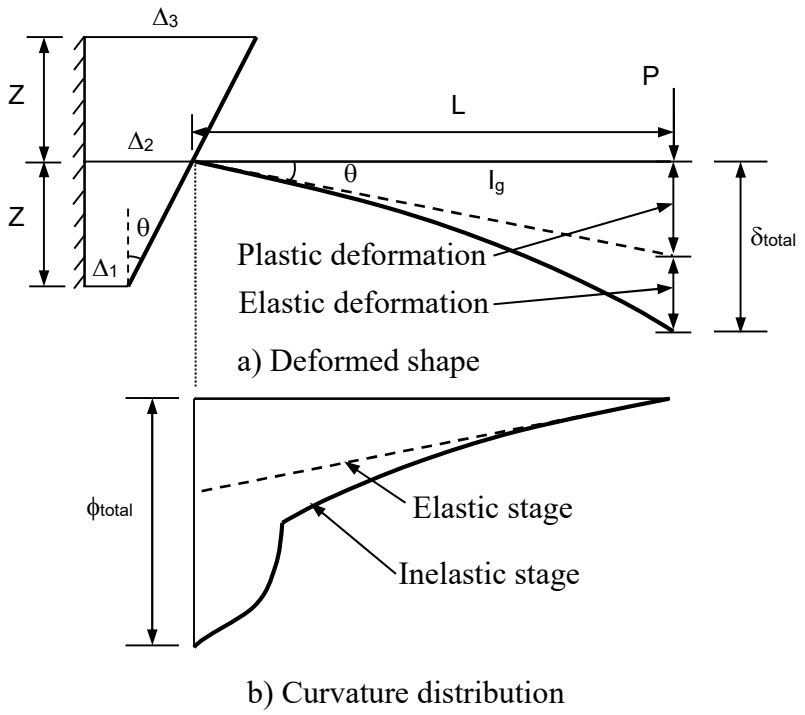

Fig. 5. Deformed shape and curvature distribution of a RC flexural member.

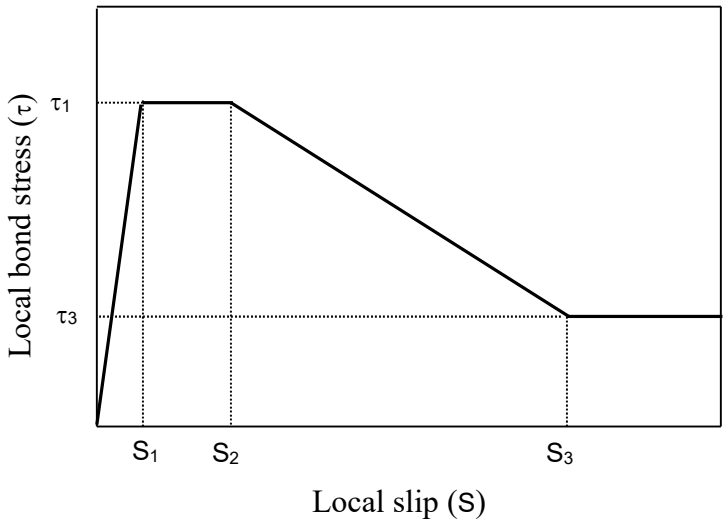

Fig. 6. Local bond stress-slip constitutive model.

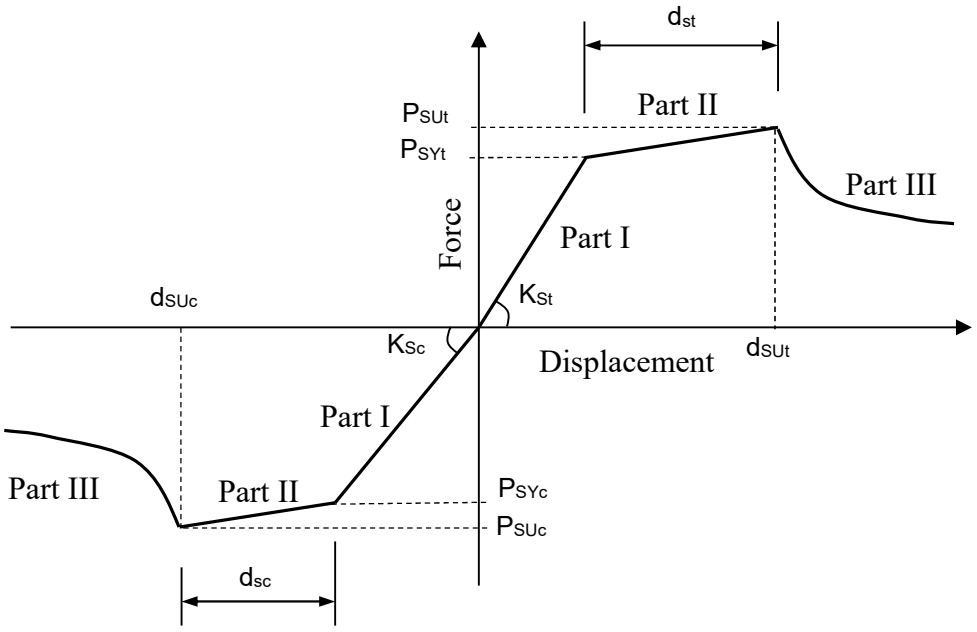

Fig. 7. Typical steel spring.

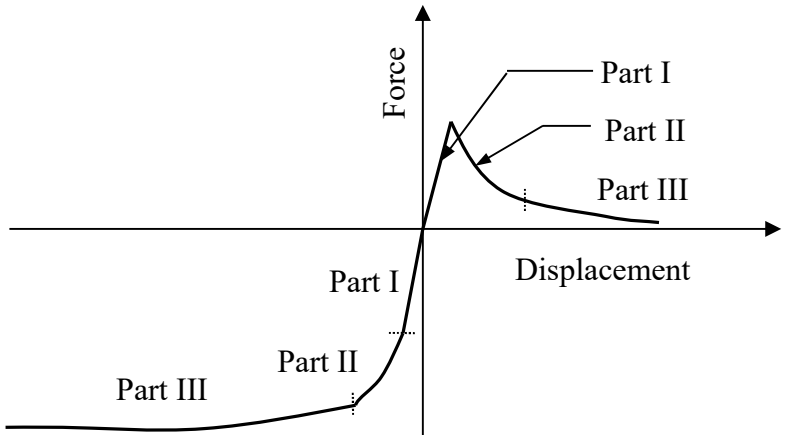

Fig. 8. Typical concrete spring.

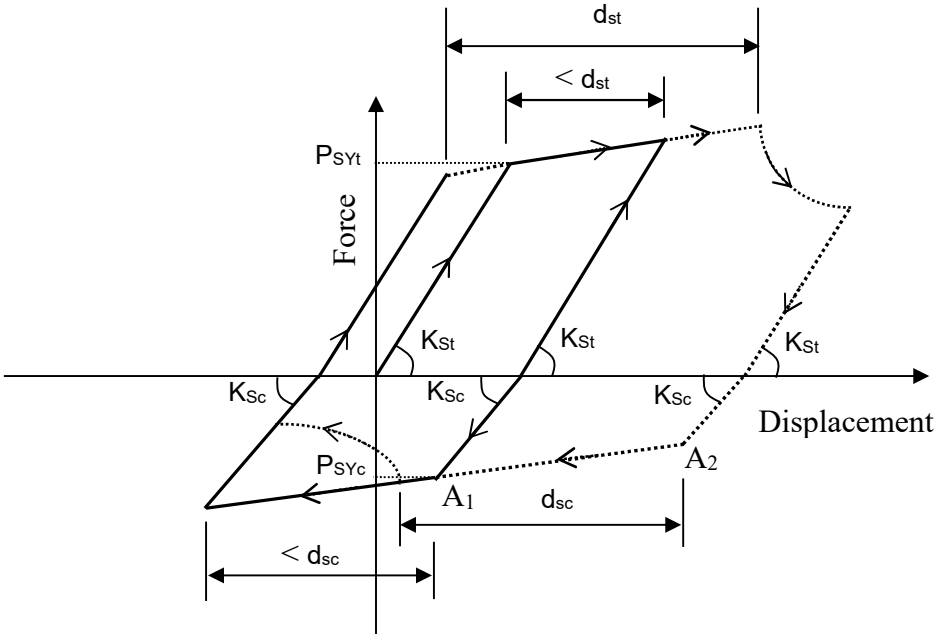

Fig. 9. Hysteretic rules for steel spring.

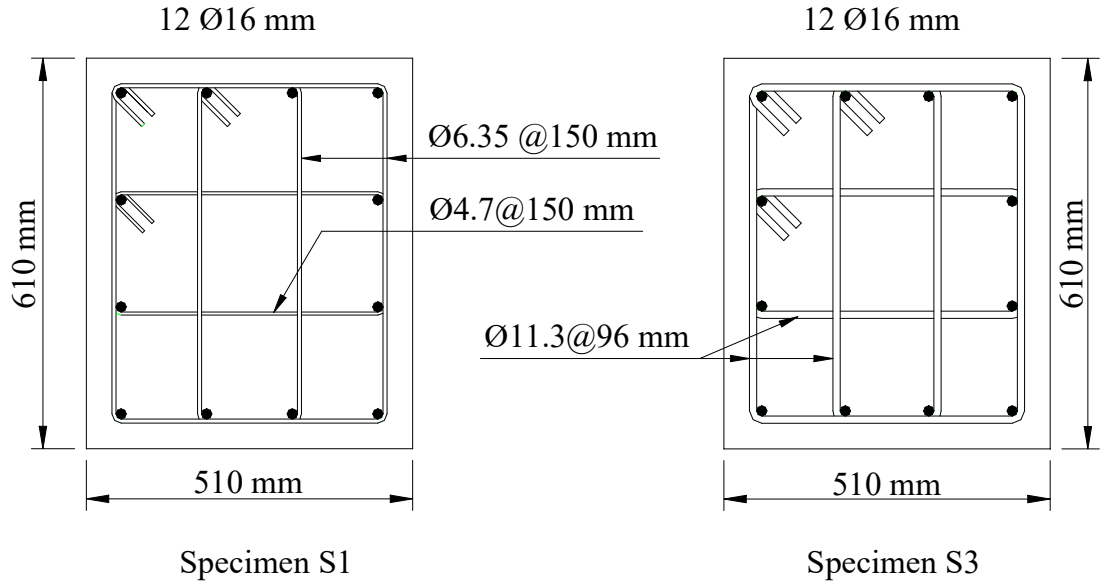

Fig. 10. Details of specimens S1 and S3.

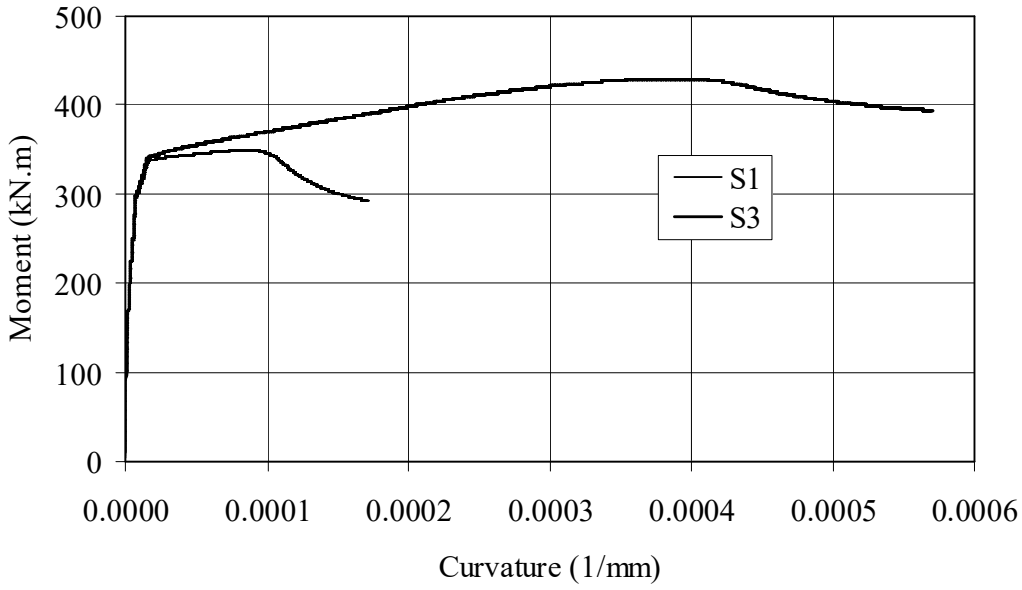

Fig. 11. Moment curvature relationships.

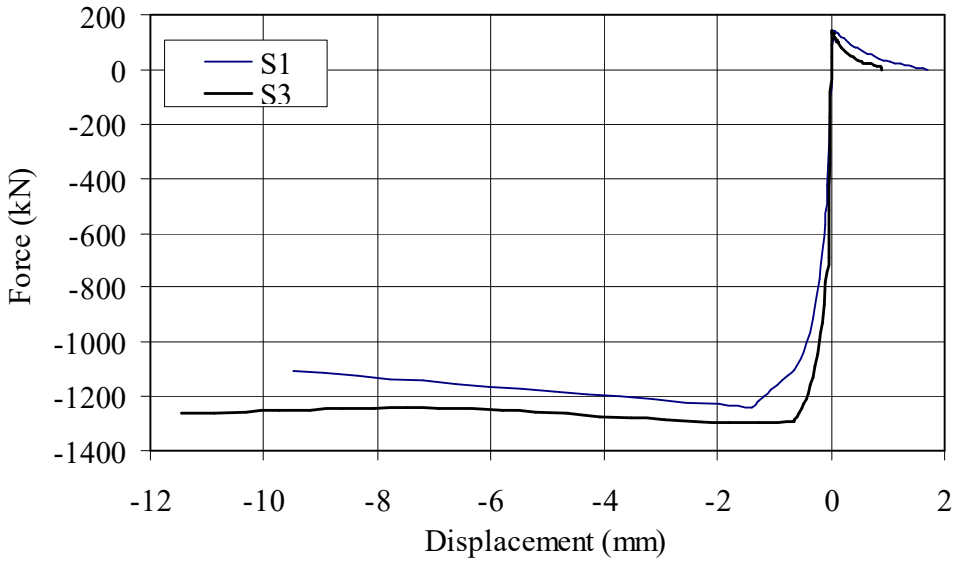

Fig. 12. Force displacement relationships for concrete springs.

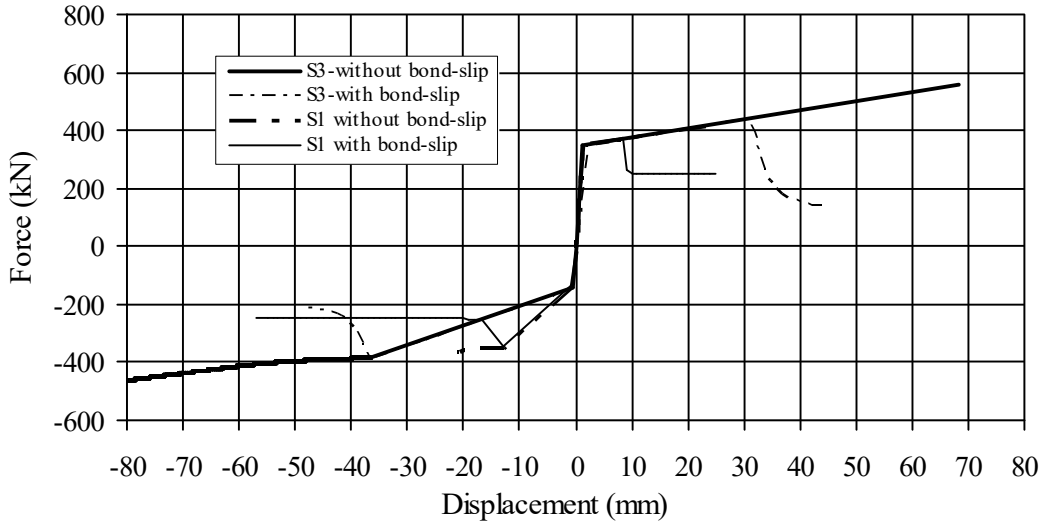

Fig. 13. Force displacement relationships for steel springs.

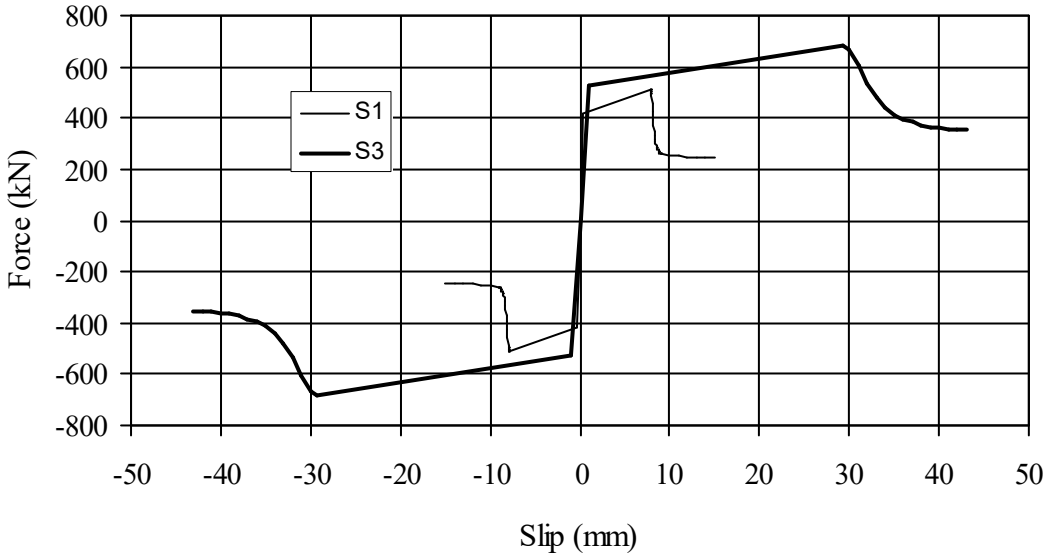

Fig. 14. Bond-slip relationships for reinforcing bars.

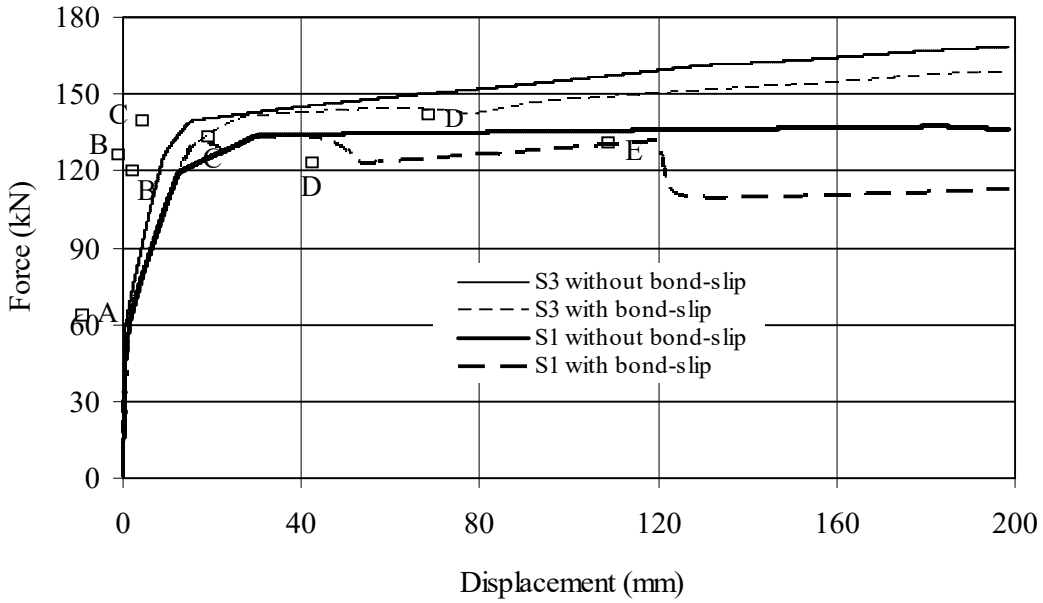

Fig. 15. Monotonic load-displacement behavior.

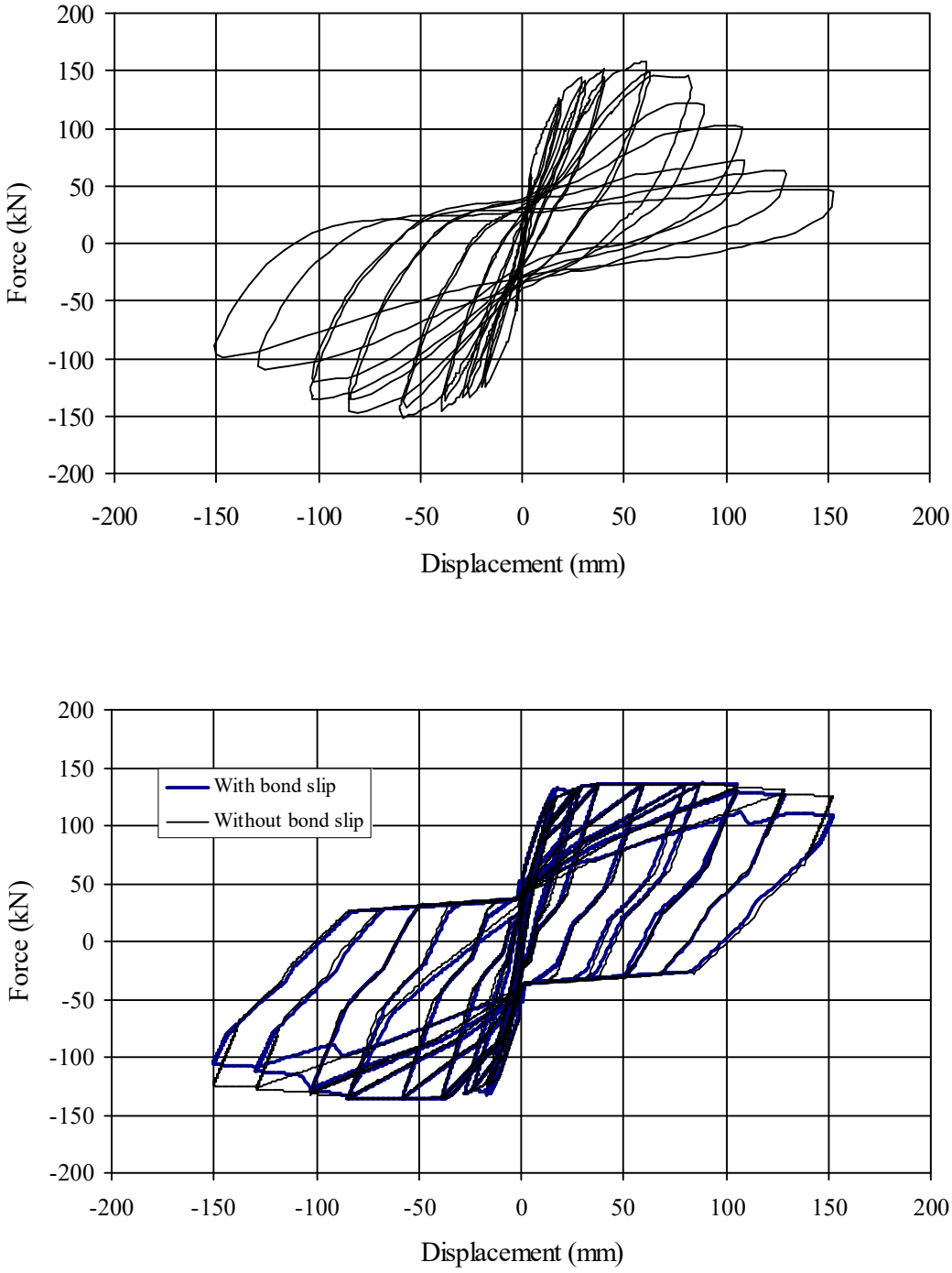

Fig. 16. Hysteretic behavior for specimen S1.
Experimental [9]

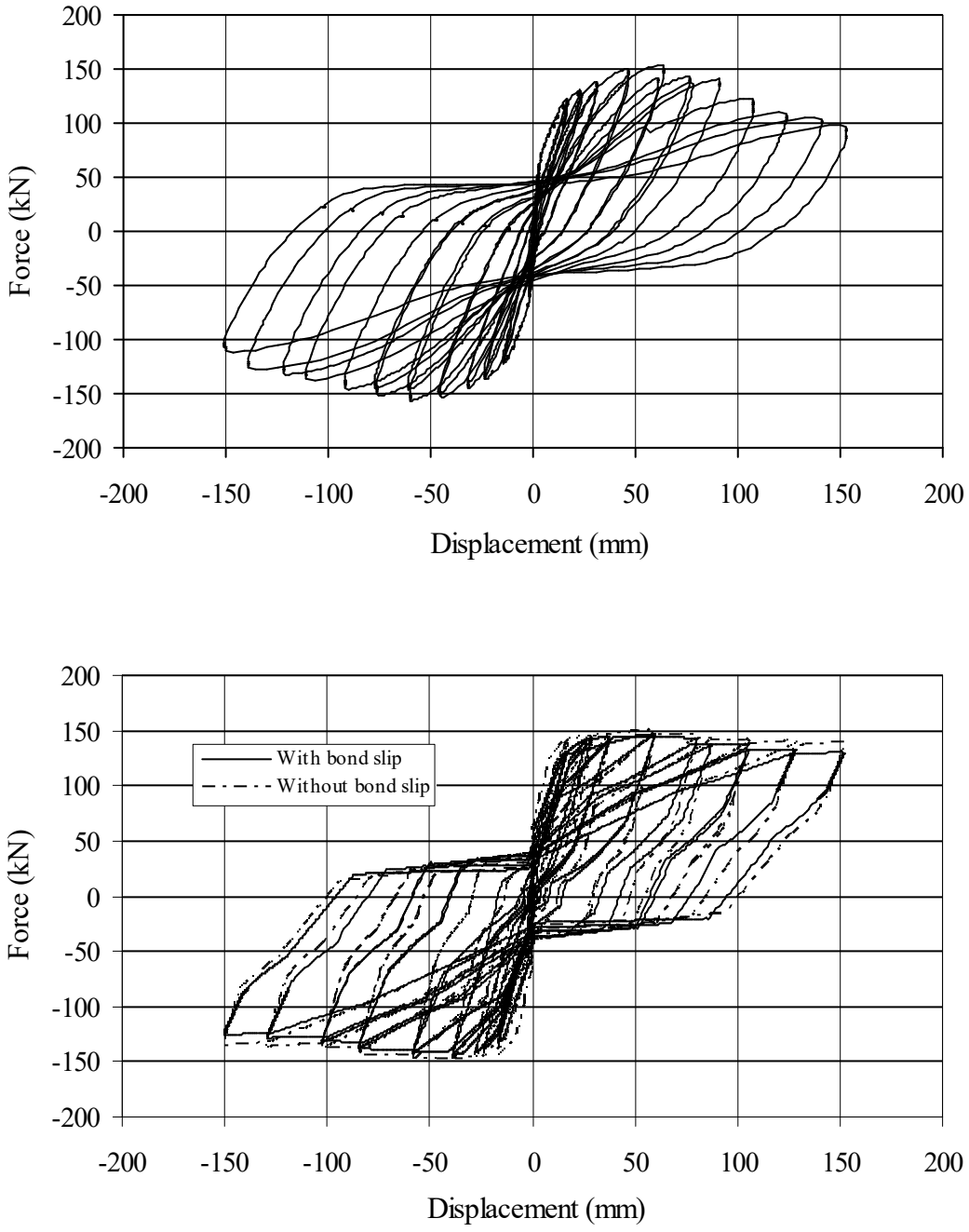

Fig. 17. Hysteretic behavior for specimen S3.

Table 1. Parameters for concrete Springs [units N and mm]

Specimen	Spring	Force Type	Portion of curve	Initial Displacement	Constants				
					K_1	K_2	K_3	K_4	K_5
S1	Exterior	Tension	II	0.0467	0.000	0.000	57.7×10^3	-185×10^3	151×10^3
			III	0.460	0.000	-25.1×10^3	114×10^3	-121×10^3	154×10^3
		Compression	II	-0.101	617×10^3	2.64×10^6	4.12×10^6	2.95×10^6	-311×10^3
			III	-1.40	0.000	0.000	0.000	-16.6×10^3	-1.26×10^6
	Center	Tension	II	0.0946	0.000	824×10^3	-1.15×10^6	609×10^3	42.1×10^3
			III	0.605	0.000	-31.1×10^3	93.9×10^3	-90.3×10^3	200×10^3
		Compression	II	-0.101	617×10^3	2.64×10^6	4.12×10^6	2.95×10^3	-311×10^3
			III	-1.40	0.000	0.000	0.000	-16.6×10^3	-1.26×10^6
S3	Exterior	Tension	II	0.0127	0.000	0.000	464×10^3	-475×10^3	146×10^3
			III	0.126	0.000	-276×10^3	531×10^3	-404×10^3	137×10^3
		Compression	II	-0.0492	0.000	2.04×10^6	3.95×10^6	2.82×10^6	-558×10^3
			III	-0.679	55.0	1.50×10^3	12.6×10^3	27.8×10^3	-1.28×10^6
	Center	Tension	II	0.0744	0.000	351×10^3	-694×10^3	486×10^3	90.0×10^3
			III	0.525	0.000	-2.11×10^3	7.26×10^3	-37.5×10^3	222×10^3
		Compression	II	-0.0492	0.000	2.04×10^6	3.95×10^6	2.82×10^6	-558×10^3
			III	-0.679	55.0	1.50×10^3	12.6×10^3	27.8×10^3	-1.28×10^6